POWER ELECTRONICS AND DRIVES
Vol. 2(37), No. 1, 2017 DOI: 10.5277/PED170103

FREQUENCY BASED ISLANDING DETECTION METHODS IN POWER ELECTRONIC CONVERTERS*

KRZYSZTOF DMITRUK, MAREK KORZENIEWSKI, ANDRZEJ SIKORSKI

Bialystok University of Technology, Department of Power Electronics and Electric Drives, ul. Wiejska 45D, 15-351 Białystok, Poland, e-mail addresses: k.dmitruk@doktoranci.pb.edu.pl; m.korzeniewski@pb.edu.pl; a.sikorski@pb.edu.pl

Abstract: Frequency based methods developed to detect an islanding condition in modern power grid structures have been discussed. The condition may occur in power grid lines to which additional energy sources with power electronic converters have been connected such as solar panels or wind turbines. It is a hazardous operating state for grid workers and devices connected to the islanded part of the grid. Such a state results from the inability to control amplitude and frequency of basic harmonic of the grid voltage. An islanding problem in a power grid with additional small energy sources has been discussed. A basic passive and active islanding detection method have been presented and compared with known frequency based algorithms, namely active frequency drift and active frequency drift with a positive feedback algorithm. Finally, a laboratory test of the proposed islanding detection methods in a three--phase grid with an AC-DC converter has been conducted. To demonstrate differences between the tested methods, total harmonic distortion injected into the output converter current and detection time of islanding state have been measured.

Keywords: *anti-islanding protection, active frequency drift, grid converter*

1. INTRODUCTION

A dynamically developing sector of renewable energy sources (RES) has a significant impact on the structure of the power grid system [1]. Currently, there is a considerable number of RES used in the grid, e.g., various types of fuel cells, solar panels or wind turbines. Grid connected small power sources called distributed generation (DG) decentralize power systems as shown in Fig. 1. In the presented structure, it is possible to electrically isolate a part of a distributed network from the main utility source. An islanding state may occur only when additional energy sources are present in an isolated network. In most applications, in order to connect DG to the power grid, grid converters are used. This method of coupling energy sources to the rest of the grid possesses a lot of advantages and disadvantages which depend on the applied control algorithm. A great

*Manuscript received: December 24, 2016; accepted: May 28, 2017.

number of converters are controlled by simple unity power factor algorithms, where a precisely measured utility voltage signal is necessary for proper operation of the converter. With a disconnected main power supply, these converters are unable to control voltage and frequency of fundamental harmonic. In such a situation, the converter should discontinue supplying the occurred island, owing to a possibility of hazard for line workers or devices connected to the island [2].

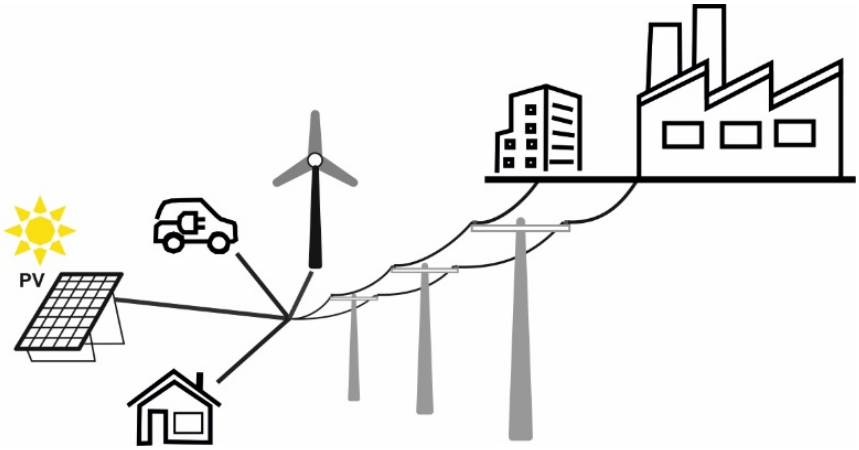

Fig. 1. Power grid with renewable energy sources

The mentioned hazard may have an impact on devices connected to the island due to changes in magnitude and frequency of line voltage in the islanded grid part. Also, line workers may be exposed to deadly danger. If they disconnect the main power supply manually, islanded part may be still energized by a renewable energy source. Another aspect that proves the necessity to use anti-islanding protection is preventing the grid converter damage. It is possible when during islanding, the main power supply will be reconnected without previous synchronization.

2. ISLANDING STATE

Let us consider an exemplary schematic of the power grid shown in Fig. 2. Between the local energy source (LES) and point of common coupling (PCC) there is a grid converter controlled by a unity power factor algorithm. As a local load, a pure resistive model is considered. In this case:

$$P_{\text{inv}} \neq 0,\ P_{\text{load}} \neq 0,\ Q_{\text{inv}} = Q_{\text{load}} \approx 0 \tag{1}$$

The pure resistive model of the islanded load is easy to identify. Moreover, it allows making power balance condition in a simple way, when the unity power factor control is implemented into the microprocessor.

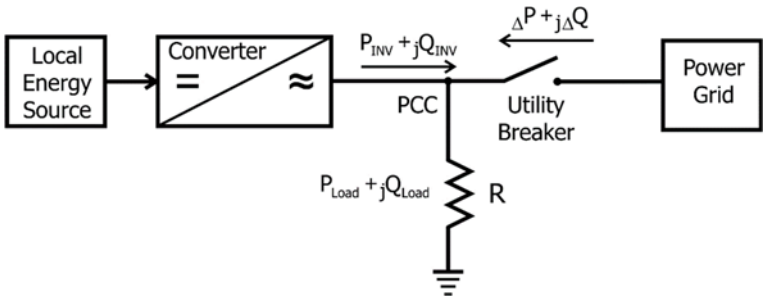

Fig. 2. Exemplary block diagram of a power grid with RES

Normal state operation occurs when the utility breaker is closed. In this state, the power generated in LES flows through the converter to PCC and next the power flows to local load. According to Fig. 2, power balance at PCC can be expressed by the following equations:

$$\Delta P = P_{\text{inv}} - P_{\text{load}}, \quad \Delta Q = Q_{\text{inv}} - Q_{\text{load}} = 0 \tag{2}$$

During a closed state of the utility breaker, the power is balanced by a power grid. The voltage and frequency are stiffly controlled by the power grid. If the breaker opens, the power flow through the breaker contacts becomes zero. In this case, there are two possible scenarios dependent on the power fed by utility at the instant before the island occurs. In the schematic in Fig. 2, ΔQ is always equal to zero, so there is no change of the frequency after grid disconnection [2]. Real power in the islanded grid part influences the voltage, due to Ohm's law. Hence, after grid disconnection, there are two possible scenarios:

- $\Delta P = 0$ – voltage remains at the same level, equal to the level prior to the opening of the switch,
- $\Delta P \neq 0$ – there is a change in the voltage level at PCC during switching operation.

A relationship between generated power and voltage in an islanded grid may be defined as follows [3]:

$$U' = U\sqrt{\frac{P_{\text{inv}}}{P_{\text{load}}}} \tag{3}$$

where U is the voltage at PCC instant before islanding state occurrence, U' – voltage at PCC instant after occurrence of the islanding state.

3. PASSIVE ANTI-ISLANDING METHOD

The analysis of Eq. (3) shows a possibility to detect the islanding operation state by observing the voltage changes at PCC. The methods based on measuring and analysis of grid parameters are called passive methods. They are commonly attained by setting threshold values for the measured voltage and frequency parameters at PCC. If the measured values exceed the set limits, the converter stops supplying the load. It should be noted that every grid-connected energy source is required to have protection units against over/under voltage protection (OVP/UVP) and over/under frequency protection (OFP/UFP).

Since there is a significant power mismatch between LES and local load, in most cases the above protection units are sufficient to prevent islanding. On the other hand, there is possibility to get perfect power balance between LES and load in the isolated part of grid. Verhoeven assesses the probability of a balanced condition in a certain part of 10^{-6}–10^{-3} [4]. Regardless of the probability, the protection should detect network disconnection under any conditions to guarantee safety.

In the case when the utility breaker opens and $\Delta P = 0$, the voltage protection unit will not recognize an emergency state. In other words, the load stays inside the non-detection zone (NDZ) [5]. In the light of the requirements of the Polish power grid law [6] and other international standards [7], the tolerance of the RMS voltage level in a normal operation state of the power grid is wide-ranging (at least ±10%). Due to this wide range of voltage tolerance, to exceed voltage thresholds in order to accomplish anti-islanding protection, a major power mismatch is required [2]. It is a generally known disadvantage of passive anti-islanding algorithms.

4. DETECTION OF THE ISLANDING OPERATION STATE BY FREQUENCY BASED ACTIVE METHODS

To minimize the main weakness of the passive method, the active methods are used in order to verify grid presence. This verification is especially important when dealing with the power match between the power generated in LES and the power consumed by the load. The current generated at the converter output can be described by the following equation:

$$i_{\text{inv}} = I_{\text{inv}} \sin\left(\omega t + \phi\right) \tag{4}$$

As seen, there are three current parameters that may be varied: amplitude, frequency and phase. Numerous authors [3, 8, 9] consider the frequency based methods to be the most reliable.

The basis for all types of frequency based methods has been the active frequency drift (AFD) algorithm. This method is based on injecting a distortion into a reference waveform (i^*) of the converter output current, as shown in Fig. 3. Perturbation of i^* is realized by generating the current reference waveform with a slightly higher frequency than the frequency of the measured voltage at PCC. Moreover, additional zero time (t_z) between two halves of periods of current reference is injected. Zero time is constant and is related to the chopping fraction parameter (cf) by a simple equation:

$$cf = \frac{t_Z}{t_{Upcc}} \tag{5}$$

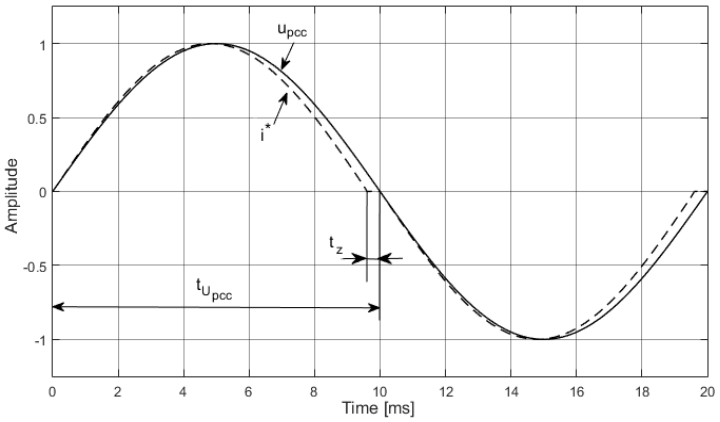

Fig. 3. Voltage at PCC and converter output current reference i^* waveforms in a basic version of the AFD method

It must be remembered that zero time is controlled only after the first half of the current reference period. Both waveforms presented in Fig. 3 start at the same time. The frequency of current waveform reference for each new cycle is calculated at the start of every new voltage period. For this reason, if frequency voltage at PCC increases during the generated cycle i^*, the voltage period becomes shorter. Hence, the next cycle of the current reference waveform will start earlier, unlike in situations when there is no change in voltage frequency. The above mechanism makes it possible to force frequency drift in the case when the utility is disconnected. This also activates an OFP unit. An additional important condition providing proper operation of the AFD algorithm is the implementation of a fast and high accuracy phase locked loop into the converter control unit.

To obtain the waveform i^* shown in Fig. 3, the authors propose a calculation method illustrated with the diagram shown in Fig. 4.

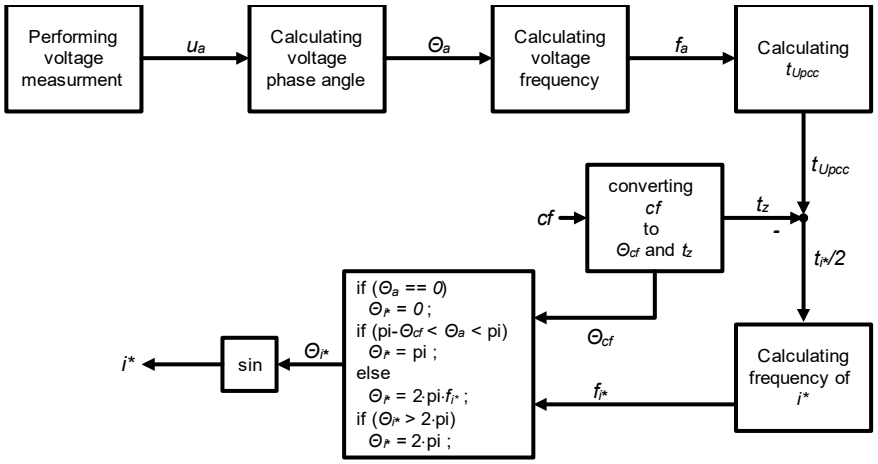

Fig. 4. Block diagram of the algorithm used in calculation of the distorted i^* in the basic AFD method

The grid converter generates an output current i correspondingly with the reference waveform i^*. As long as the power grid remains connected, there is no influence of the distorted current to voltage waveform at PCC (u_{pcc}). When the utility breaker opens, u_{pcc} depends on i. If the measured voltage frequency increases, the converter current frequency is also increased to keep constant *cf,* which is predetermined. This process of frequency changes repeats until the OFP threshold is exceeded, which is a sufficient condition to stop the power electronic converter.

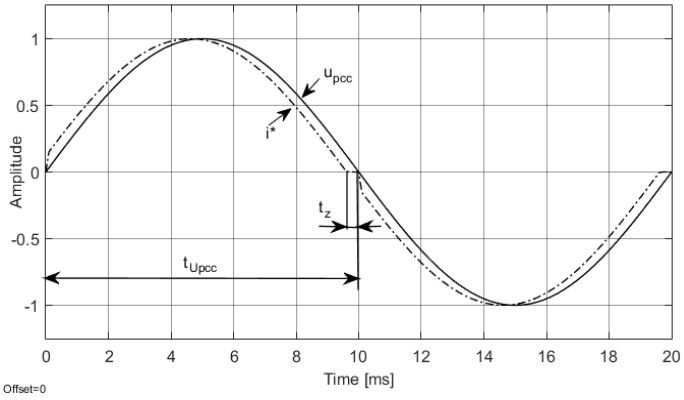

Fig. 5. Voltage at PCC and converter output current reference i^* waveforms in the modified version of the AFD method

In [2], [10] and [11], the authors describe a main drawback of the basic AFD method, which is a high level of total harmonic distortion in the output converter current. Due to constant value of *cf*, the power converter generates a distorted current during the entire

converter operation time. Chopping fraction, i.e., *cf* is set to values higher than 0.015 in order to obtain a reliable anti-islanding protection with different types of local load [2]. Illustrative waveforms obtained from the simulations shown in Fig. 3 and Fig. 5 have *cf* set to 0.04.

To obtain shorter time of islanding state detection, *cf* must be increased. On the other hand, the value of *THD* limits the range of useful *cf* values. This restriction is imposed to prevent the distortions to reach their maximum values allowed by the power grid law [7]. In paper [10], to solve the problem of high current distortions, a modification of the distortion injected into i^* was proposed. The modified waveform is presented in Fig. 5 below.

In comparison to the method shown in Fig. 3, some significant changes can be seen here. Frequency of voltage u_{pcc} and i^* are equal. To obtain adequate duration of zero time specified by predefined *cf*, a calculation of phase angle offset is performed. The reference waveform i^* shifted in phase reaches zero level at time $t = t_{Upcc} - t_z$. All the required calculations are performed at positive zero crossing of u_{pcc} waveform. To reproduce a modified current waveform proposed in [10], we proposed an algorithm shown in Fig. 6.

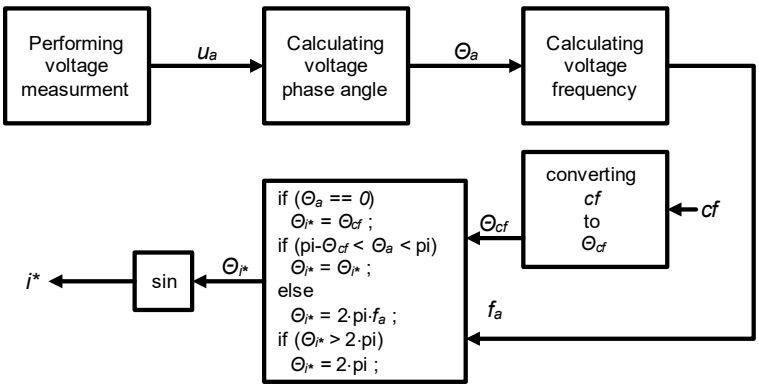

Fig. 6. Block diagram of the calculation algorithm to reproduce distorted i^* in the modified AFD method

To compare described AFD algorithms, a simple simulation was carried out. Parameter *cf* was set to value 0.04 for both methods. Total Harmonic Distortion (THD_{40}) for the waveforms was calculated in Simulink. The computed THD_{40} values for the basic method is 4.01% and 1.90% for the modified AFD method. This calculation proves that a lower level of THD_{40} can be achieved by modifying the injected distortion into i^* waveform. It is a very important conclusion in view of another disadvantage of AFD methods described in [2] and [8]. The disadvantage involves a long time required to detect an islanding condition when *cf* is reduced to fulfil *THD* limits. To solve this problem, various modifications of the basic method was proposed [2], [6]. Most of them

change the value of *cf* parameter during the process of frequency drift after grid disconnection. For this purpose the methods make use of positive feedback with linear gain function *K* of voltage frequency error Δf.

$$\Delta f = f_0 - f_a \tag{6}$$

$$cf = cf_0 + K(\Delta f) \tag{7}$$

Parameter cf_0 is predefined and equal to *cf* used in equation (5), f_0 is a nominal value of grid frequency, f_a is actual frequency of voltage measured at PCC.

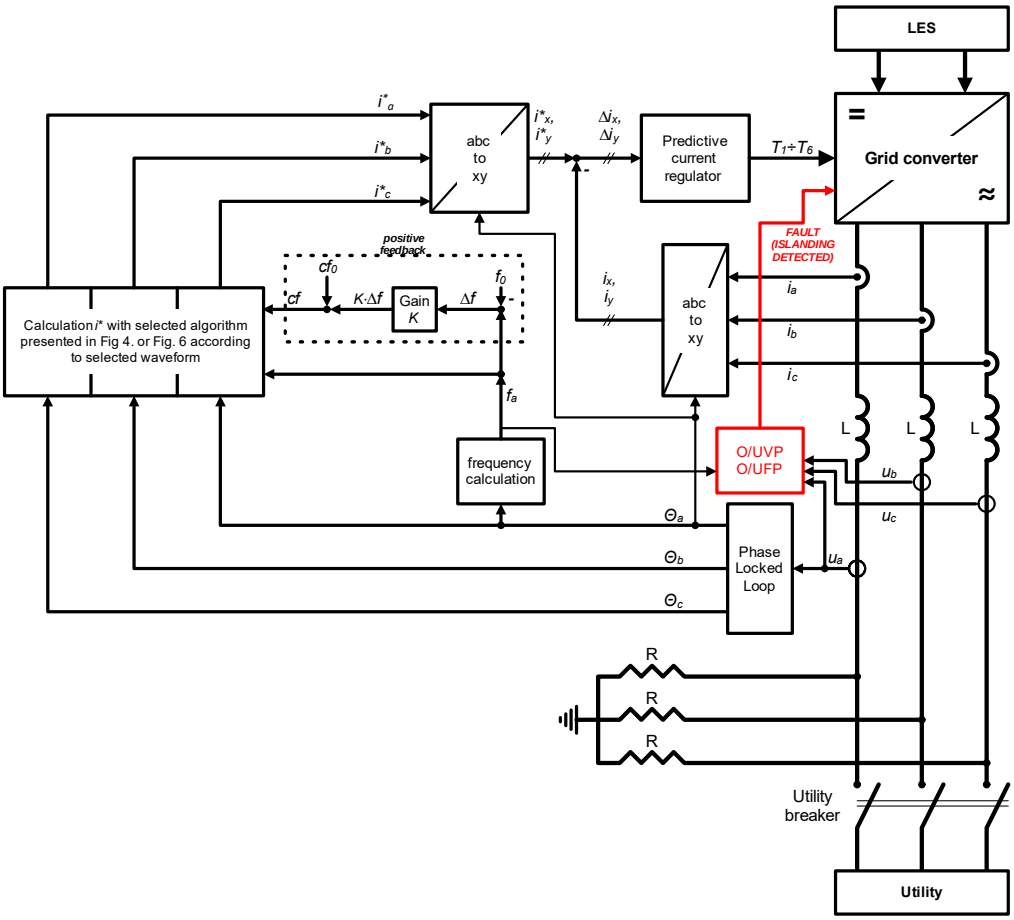

Fig. 7. Implementation of AFDPF algorithm into converter control unit

The AFD method described in [2] uses a positive feedback mechanism and has been called Active Frequency Method with Positive Feedback (basic AFDPF – in this article

it is called basic, because it was first known method of realisation anti islanding protection with adjusting frequency). Implementation of variable *cf* allows to reduce a converter output current distortion in the case when the grid is connected and also shortens the detection time of island condition [2], [5]. Reduction of the *THD* level in *i* in steady state is an effect of using lower values of *cf* when the power grid is connected. After utility disconnection or utility breaker opening, even a small disturbance injected into *i* causes a difference between nominal and actual value of voltage frequency. The detected error is gained by factor *K,* which increases *cf*. A higher value of *cf* causes an increase of Δf, hence *cf* is amplified again. This positive feedback mechanism is repeated many times until the frequency protection activates and shuts off the power electronic converter.

Chen et al. [10] proposed a new output waveform but only with constant *cf*. In this paper, the authors propose a modification by adding a positive feedback mechanism with linear function of voltage frequency error in order to calculate i^* waveform proposed in [10]. Here the calculations were performed using Eqs. (6) and (7). This modification should shorten the island condition detection time in comparison to the basic AFDPF method that uses the waveform presented in Fig. 3. The implementation of the algorithm into the converter control unit and a laboratory test circuit is shown in a block diagram (Fig. 7).

The outer regulation loop contains a phase locked loop which generates three phase angles from a single phase voltage measurement. Additionally, the loop also contains a block that calculates selected waveforms. The inner regulation loop regulates output converter currents in synchronous rotating reference frame *xy* by using a predictive current controller. The properties and performance of the used regulator are described in [12].

5. LABORATORY TESTS

To investigate the theoretical results, laboratory tests have been carried out. A schematic diagram of the first tested circuit is presented in Fig. 8.

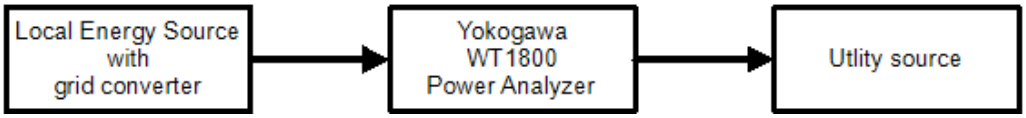

Fig. 8. Schematic diagram used to test total harmonic distortion

The two methods with constant *cf* mentioned in the third section have been implemented into the microprocessor based controller of a DC/AC grid converter. The converter is controlled by a high performance 32-bit floating point SHARC processor

(ADSP-21369). Clock frequency is set to 350 MHz. The execution time of the developed anti-islanding algorithm is 2.0 μs.

The amount of the generated power is constant during the test and stays at 3.8 kW. The measurement of THD_{40} is performed with Yokogawa 1800WT power analyser. In the case of utility presence, THD_{40} in the function of variable *cf* is presented in Fig. 9.

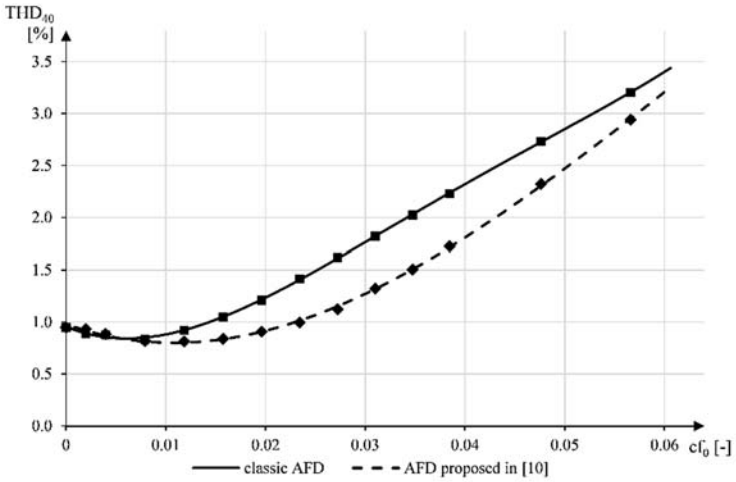

Fig. 9. THD_{40} in converter current output for two tested methods in function of *cf*

As can be seen, the laboratory test proves that the modified AFD algorithm presented in [10] injects smaller distortions into the converter output current. Over the entire range of *cf*, maximum difference between the curves presented in Fig. 9, for $cf = 0.035$ is about 0.52%. The calculated reduction of the injected distortion into the converter current is equal to 34.58% ($cf = 0.035$). Chen et al. [10] performed a simulation test to obtain *THD* of the converter output current. They concluded that their method lowered the *THD* by about 90% compared to the basic AFD method with the same input parameters (*cf*) for both methods. To confirm that result we carried out a simulation test. The measured distortions in the output current were equal to 4.01% of *THD* in the basic method and 1.90% in the modified AFD method ($cf = 0.04$). Reduction in the THD current in the simulation test was ca. 52%. These results do not confirm the results obtained by Chen et al. [10].

Another test was performed to obtain a spectrum of the analyzed converter output currents. As shown below, the basic AFD method increases the 5th harmonic twice, the 7th harmonic is 5.3 times higher than the values of the same harmonic in current *i*, during the converter operation without implemented anti-islanding detection. On the other hand, the modified AFD algorithm significantly increases the 3rd, 29th and 35th harmonic (about twice) and the 17th as well as 23rd (about 2.5 times).

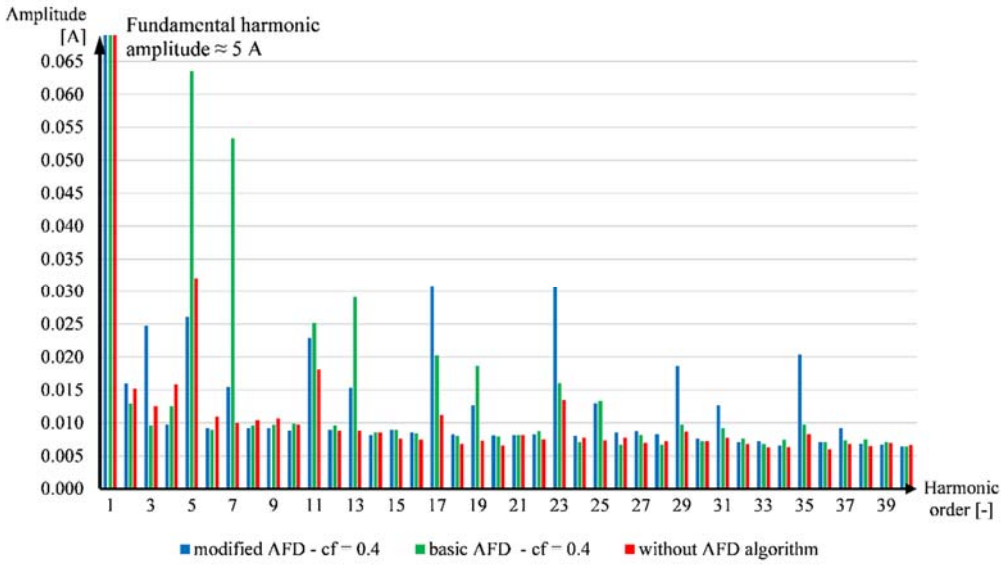

Fig. 10. Spectrum of converter output power

An exemplary waveform of converter output current for typical *cf* value for AFD algorithms with positive feedback are presented below (*cf* = 0.025). Fig. 11 shows that the injected zero time is a very small part of power grid voltage period (about 250 μs), in the case when the power converter is connected with the utility.

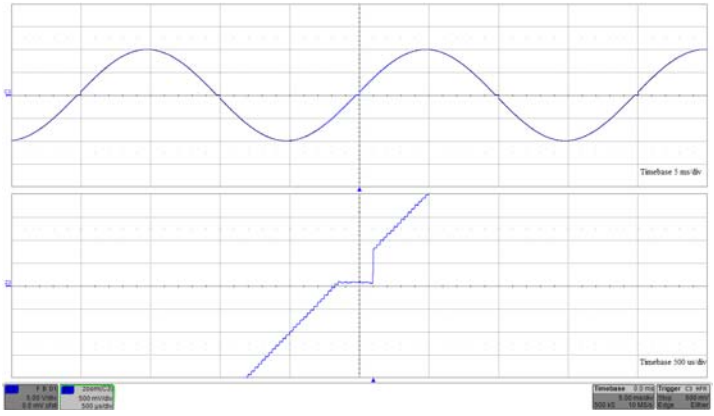

Fig. 11. Converter output current reference waveform for *cf* = 0.025 (AFD waveform proposed in [10]). Lower part shows a magnified part of the waveform in the upper part

Apart from the THD_{40} measurements also the detection time (t_d) of island condition in function of cf_0 and K have been performed. The laboratory test was carried out with

the implemented basic AFDPF method [2], and the AFD method with the waveform [10] with the modifications introduced by the present authors. The second laboratory test circuit was improved to the setup shown in Fig. 7. The circuit specification is given Table 1.

Table 1. Laboratory circuit parameters

Parameter	Value
Grid voltage	230 V
Grid frequency	50 Hz
Filter inductance (L)	15 mH
Load power	1.8 kW
Frequency threshold in OFP	0.5 Hz

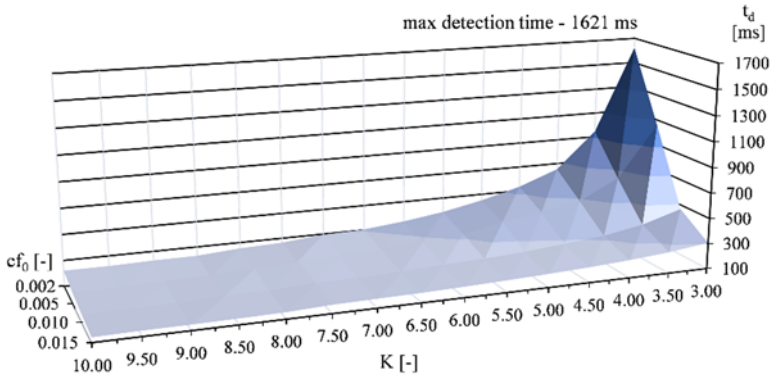

Fig. 12. Required time to detect occurred island with basic AFDPF method

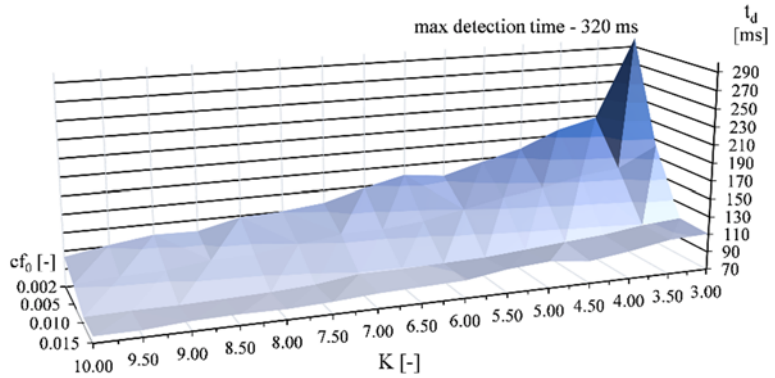

Fig. 13. Required time to detect occurred island with proposed AFDPF method

The oscilloscope measurements were performed with respect to current and voltage waveforms. The measured time was a period between the opening of the utility breaker

and tripping of the frequency protection unit. During the test, the performance of both algorithms was verified in the function of various combinations of input parameters. The results in Fig. 12 and Fig. 13 show a major difference between the required time to detect an occurred island condition in the power grid. The results depend not only on parameter settings – an important issue is the implemented current waveform distortion.

During the laboratory tests, exemplary waveforms were recorded to show dynamic changes *cf*. Parameters cf_0 and K were tuned to record the whole process of island detection in the time range 120–170 ms.

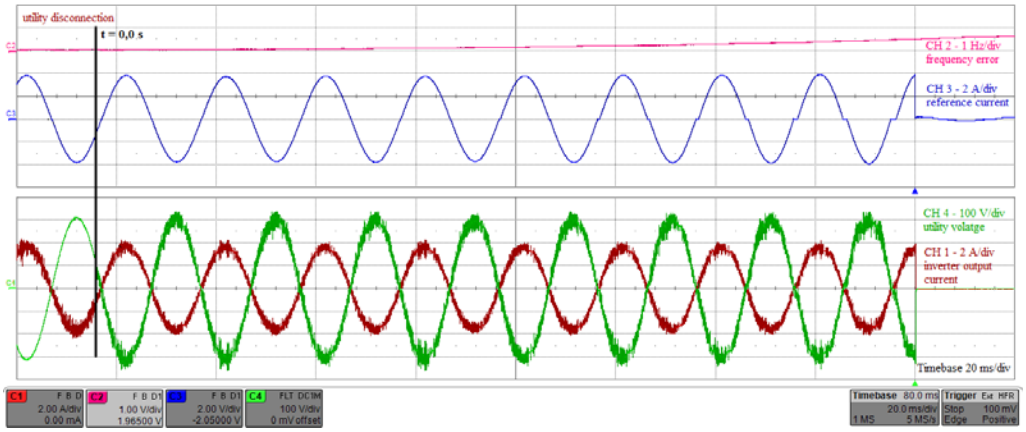

Fig. 14. Converter output waveforms in basic AFDPF method (cf_0 = 0.01 and K = 10)

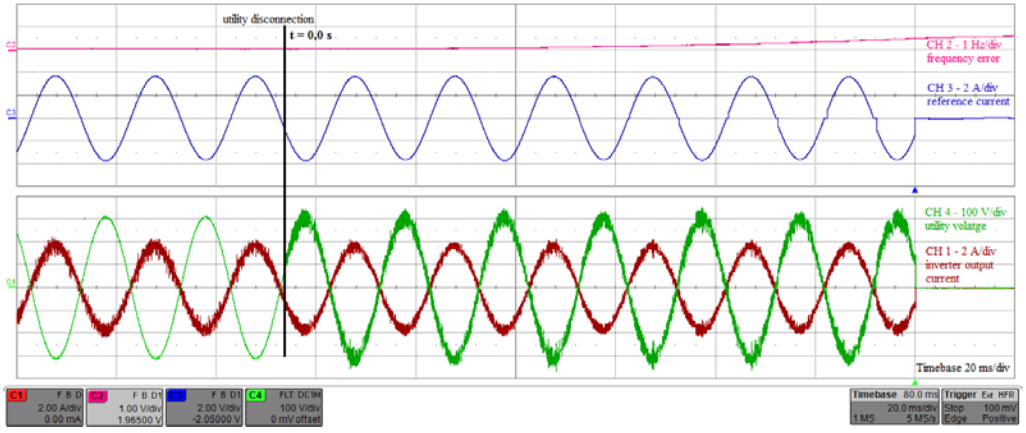

Fig. 15. Converter output waveforms in proposed AFDPF method (cf_0 = 0.01 and K = 5)

The results presented in Fig. 14 and 15 show dynamic changes of *cf* parameter after utility disconnection. The changes can be seen analysing the blue waveform of the converter

reference current (CH3). After utility disconnection at time 0.0 s (the vertical black line), the frequency error is increases. According to equation (6), zero time becomes longer for each next period of the utility voltage. In the proposed AFDPF method, to achieve the same detection time in comparison to the basic AFDPF method, there is a need to set only half value of K parameter, when cf_0 stays at the same level. It allows us to generate lower level of *THD* at the converter output during the process of islanding detection.

6. CONCLUSION

Final analysis of the AFDPF methods discussed here let us formulate two main conclusions. In order to achieve the same time of island state detection, there is a possibility to use higher K and lower cf_0 or higher cf_0 and lower K values. By tuning these parameters, there is a possibility to influence total harmonic distortions in power converter output current, especially in the case when the converter cooperates with the utility. Lower cf_0 values reduces current *THD* (Fig. 9), but also extends the detection time when the islanding occurs. This negative effect can be successfully compensated by tuning K to higher values. The results also show that frequency based anti-islanding detection algorithms can be tuned in a narrow range of input parameters to adjust the detection time in a wide range.

Considering the AFD algorithms without positive feedback, we can state the following: injection of various distortion waveforms into converter output current has a significant impact on the generated *THD* of the current, for example: an introduction of a modified reference current waveform an approximate 30% reduction of *THD* in output current can be achieved in a real electric circuit. Moreover, this distortion in comparison to the basic version of the AFD method amplifies higher harmonic orders (17th, 23th, 29th, 35th) that can be easily filtered out.

The above knowledge may be used in the designing of high effective, reliable anti-islanding protection systems characterized by reduced total harmonic distortions injected into converter output current.

ACKNOWLEDGEMENTS

The work was supported by the research project S/WE/3/2013 funded by the Scientific Subsidy of the Ministry of Science and Higher Education (MNiSW).

REFERENCES

[1] WŁAS M., *Distributed generation in power supply system*, Zeszyty Naukowe Wydziału Elektrotechniki i Automatyki Politechniki Gdańskiej, 2010, No. 27, 39–42.

[2] ROPP M., BOWER W., *Evaluation of islanding detection methods for utility-interactive inverters in photovoltaic systems*, Sandia National Laboratories, US, November 2002.

[3] SKOCIL T., GOMIS-BELLMUNT O., MONTESINOS-MIRACLE D., GALCERAN-ARELLANO S., RULL-DURAN J., *Passive and active methods of islanding for PV systems*, 13th European Conference on Power Electronics and Applications, Barcelona, Spain, 2009, 1–10.

[4] VERHOEVEN B., *Probability of islanding in utility network due to grid connected photovoltaic power systems*, Report of the International Energy Agency – Phtovoltaic Power Systems Programme T5-07:2002, September 2002.

[5] ROPP M., BEGOVIC M., ROHATGI A., KERN G.A., BONN R.H. GONZALES S., *Determining the reflective effectiveness of islanding detection methods suing phase criteria and nondetection zones*, IEEE Trans. Energy Conv., 2000, 15(3), 290–296.

[6] Polish Standard PN-EN 50160:1998. *Voltage characteristics in public distribution systems, Poland.*

[7] SCHWARTFEGER L., SANTOS-MARTIN D., *Review of distributed generation interconnection standards*, Proc. EEA Conference Exhibition, 18–20.06.2014, Auckland, New Zealand.

[8] PERSSON D., *Islanding detection in power electronic converter based distributed generation*, M.Sc. Diss., Lund University, 2007.

[9] TEOH W.Y., TAN C.W., *A comparative study of anty-islanding control techniques for grid-connected photovoltaic systems*, The World Congress on Advanced in Nano, Biomechanics, Robotics, and Energy Researches, Seoul, Korea, 2013, 889–917.

[10] CHEN W., WANG G., ZHU X., ZHAO B., *An improved active frequency drift islanding detection method with lower total harmonic distortion*, Proc. IEEE Energy Conversion Congress and Exposition, Denver 2013, 5248–5252.

[11] YAFAOUI A., WU B., KOURO S., *Improved active frequency drift anti-islanding detection method for grid connected photovoltaic systems*, IEEE Trans. Power Electr., 2012, 27(5), 2367–2375.

[12] FALKOWSKI P., SIKORSKI A., *Predictive control of active power of AC/DC converter with constant average switching frequency*, Przegl. Elektr., 2013, 89(12), 53–56.